colloids and interfaces

MDPI

Article

An Imine-Based Two-Dimensional Covalent Organic Framework for Gemcitabine Delivery

Kajal Kaliya [1,2], Neha Bhardwaj [1,2], Ruchika [1,2] and Ankit Saneja [1,2,*]

[1] Formulation Laboratory, Dietetics and Nutrition Technology Division, CSIR-Institute of Himalayan Bioresource Technology, Palampur 176061, India; kaliakajal2@gmail.com (K.K.); nehabhardwaj.2011@gmail.com (N.B.); ruchika.ihbt20a@acsir.res.in (R.)
[2] Academy of Scientific and Innovative Research (AcSIR), Ghaziabad 201002, India
* Correspondence: ankitsaneja@ihbt.res.in or ankitsaneja.ihbt@gmail.com; Tel.: +91-1894-233339 (ext. 485)

Abstract: A 2D imine-linked covalent organic framework (COF) with good biocompatibility was synthesized using o-Dianisidine and 1,3,5-Triformylbenzene. The synthesized COF was characterized by using the Fourier transform infrared (FTIR), thermogravimetry analysis (TGA), scanning electron microscopy (SEM), and transmission electron microscopy (TEM). The synthesized COF was subsequently utilized for the delivery of gemcitabine (Gem), an FDA-approved drug for the treatment of pancreatic cancer. The COF demonstrated a remarkable drug loading of 30 µg/mg and better drug release at pH 5.0. The biocompatibility of the COF was evaluated in the L929 (mouse fibroblast) cell line, while the cytotoxicity of the Gem-loaded COF (COF-Gem) was evaluated against the MIA-PaCa-2 and PANC-1 (pancreatic cancer) cell lines using MTT (3-(4,5-dimethylthiazol-2-yl)-2,5-diphenyltetrazolium bromide) assay. The results indicated that the COF was safe at concentrations up to 200 µg/mL, while the COF-Gem led to superior cytotoxicity as compared to native Gem, with IC_{50} values of 8.1 ± 1.2 µM in MIA-PaCa-2 cells and 6.0 ± 1.3 µM in PANC-1 cells after 48 h. This study offers a new perspective of utilizing COF as a promising delivery system for Gem delivery.

Keywords: covalent organic framework; biocompatibility; gemcitabine; pancreatic cancer; biomedical applications

Academic Editors: Aleksandra Szcześ, Wuge Briscoe, Reinhard Miller, Milad Radiom and Elena Mileva

Received: 25 October 2024
Revised: 16 January 2025
Accepted: 20 January 2025
Published: 21 January 2025

Citation: Kaliya, K.; Bhardwaj, N.; Ruchika; Saneja, A. An Imine-Based Two-Dimensional Covalent Organic Framework for Gemcitabine Delivery. *Colloids Interfaces* **2025**, *9*, 8. https://doi.org/10.3390/colloids9010008

1. Introduction

Cancer is one of the leading causes of death in developed nations, and the high mortality rate is largely due to the ineffectiveness of current treatment options [1]. The anticancer drugs available commercially have failed to target the diseased tissues or organ specifically and spread throughout the body, resulting in several side effects [2,3]. Moreover, the direct administration of the drugs to patient faces several challenges including poor dispersibility in aqueous solution, low targeting efficacy, inadequate cell membrane penetration, low stability, and unregulated drug delivery [4,5]. To address these limitations, nanocarriers, particularly porous materials with properties such as a large surface area, enhanced permeability, high drug-loading capacity, controlled pore sizes, and structural stability, offer a promising solution and are widely used in drug delivery systems [6]. Porous materials like covalent organic frameworks (COFs) and silica-based materials are particularly suitable candidates for targeted drug delivery [7–9].

COFs are the newly emerged crystalline porous materials made up through the covalent bonding of light elements like carbon (C), nitrogen (N), hydrogen (H), oxygen (O), boron (B), silicon (Si), and sulfur (S) [10]. These porous materials are gaining considerable

attention nowadays due to their unique properties such as structural diversity, absence of metal ions, tunable pore sizes, porous structures, high surface area, and extremely low densities [11–13]. Since their discovery by Omar Yaghi in 2005, COFs have been widely investigated for a diverse range of applications, including sensors, gas storage and separation, electrical conductivity, catalysis, electrochemical sensing, optoelectronic devices, and energy storage [14–18]. In addition to these applications, COFs show great potential for biomedical uses, particularly in drug delivery, owing to their stability, porous structures, low toxicity, and metal-free nature [19–21]. In 2015, Yan et al. reported the first application of COFs for the delivery of ibuprofen (IBU) [22]. Despite the growing number of studies on COFs, their exploration as carrier systems for drug delivery remains limited, highlighting the need for further research in this area [23].

Here, in this work, we initially synthesized an imine-linked COF via the Schiff base condensation of o-Dianisidine and 1,3,5-Triformylbenzene under solvothermal conditions. The resulting COF was characterized through FTIR, TGA, SEM, and TEM analysis. The synthesized COF was further explored for the delivery of Gemcitabine (Gem), a pyrimidine nucleoside analog. Gem is widely used, either alone or in combination with other chemotherapeutic agents or radiation therapy, to treat a range of cancers, including pancreatic, ovarian, bladder, breast, and non-small-cell lung cancers [24]. Further, Gem exhibits poor loading efficiency when entrapped into polymeric and lipid-based nanoparticles. Therefore, the primary objective of this study was to demonstrate the potential of COFs as an effective carrier system for the delivery of Gem. The drug-loading capacity of the COF was evaluated, and the in vitro release profile of Gem was thoroughly examined. Furthermore, the biocompatibility of the unloaded COF was assessed using L929 cell lines, while the in vitro cytotoxicity of the Gem-loaded COF was tested on MIA-PaCa-2 and PANC-1 cancer cell lines.

2. Materials and Method

o-Dianisidine (MW: 244.294 g/mol, Cas No: 119-90-4, Purity: > 95.0%), 1,3,5-Triformylbenzene (MW: 162.14 g/mol, Cas No: 3163-76-6, Purity: > 98.0%), Gemcitabine (MW: 299.659 g/mol, Cas No: 122111-03-9, Purity: > 98.0%), 1,4-dioxane (MW: 88.106 g/mol, Cas No: 123-91-1, Purity: > 99.0%), and acetic acid (Cas No: 64-19-7, Purity: >99.5%) were purchased from TCI. Tetrahydrofuran (MW: 72.11 g/mol, Cas No: 109-99-9, Purity: $\geq$99.9%) was procured from Sigma-Aldrich, St. Louis, MO, USA. Other than these, analytical-grade chemicals and reagents were utilized for the studies, and distilled water obtained from Millipore MilliQ®, Molsheim, France ultrapure water system was used. L929, MIA-PaCa-2, and PANC-1 (human pancreatic cancer cell lines) were procured from National Centre for Cell Science (NCCS), Pune, India, and were maintained in Dulbecco's Modified Eagle Medium (DMEM) supplemented with 10% (v/v) FBS (Gibco, Waltham, MA, USA). Cells were kept in an incubator under standard conditions of 37 °C temperature and 5% CO_2 and passaged for further experiments.

2.1. Synthesis of COF

An imine-linked COF was synthesized via Schiff base condensation of o-Dianisidine (3,3′-dimethoxybenzidine) and 1,3,5-Triformylbenzene under solvothermal condition [25]. In brief, to the mixture of 1,3,5-triformylbenzene (50 mg, 1 eq.), 3,3′-dimethoxybenzidine (112 mg, 1.5 eq.), 1,4-dioxane (3 mL) and 3M acetic acid (0.6 mL) were added in a tube under vacuum. The tube was flash-frozen in liquid N_2, and when the temperature of tube was raised to room temperature, it was placed at 120 °C for three days to form yellow precipitates. The precipitates were collected by centrifugation and washed with

tetrahydrofuran (THF) and acetone. The solid yellow precipitates formed were dried in an oven (Scientech instruments, New Delhi, India) 80 °C for 12 h [25].

2.2. Preparation of Gem-Loaded COF

The Gem-loaded COF was prepared by adding Gem (30 mg) and COF (60 mg) in 4 mL water. The mixture was vortexed for 10–15 min and stirred at 350 rpm for 72 h. After 72 h, the resulting mixture was centrifuged to collect the precipitates. The precipitates formed were washed with distilled water and dried at 50 °C for 12 h [25].

2.3. Determination of Loading Capacity of COF

To determine the drug-loading capacity of COF, 10 mg of COF-Gem was added to 1 mL of MQ water. The resultant mixture was vortexed and sonicated at 25 °C for 20 min and centrifuged (15,000 rpm at 25 °C) [25]. The supernatant was collected and evaluated for the Gem loading by using the HPLC system (Agilent 1260 Infinity II, Waldbronn, Germany) equipped with a quaternary pump (G7111A, 1260 Quat Pump VL), an automatic vial sampler injector (G7129A, 1260 Vial sampler), a multicolumn thermostat (G7116A, 1260 MCT) with C18 reverse phase column (LiChrospher® 100 RP-18 Hibar® RT, 250 mm × 4.6 mm, 5 µm, Darmstadt, Germany) for chromatographic separation, and a DAD detector (G7115A, 1260 DADWR). The HPLC analysis was performed under isocratic conditions, with a mobile phase consisting of 70% ACN and 30% TFA/water, at a flow rate of 1 mL/min.

2.4. Characterization

The Fourier transform infrared (FT-IR) spectra were recorded using Agilent Technologies (Santa Clara, CA, USA), covering a range from 4000 to 500 cm^{-1}. The thermal degradation behavior of COF, Gem, and COF-Gem was analyzed using a thermogravimetric analyzer (TGA, TA Instruments Waters, New Castle, DE, USA), model: Discovery TGA5500). TGA measurements were conducted from 30 °C to 700 °C at a heating rate of 20 °C/min. The experiments were carried out in sealed aluminum pans, with an empty pan serving as a reference. The morphology of COF and COF-Gem was examined using a scanning electron microscope (SEM, Hitachi S-3400N, Tokyo, Japan). In brief, the COF was evenly spread on a double-sided adhesive carbon tape attached to a 25 mm metal stub. The sample was sputter-coated with gold using an ion sputter coater (Hitachi-1030, Tokyo, Japan) to enhance conductivity. SEM micrographs were captured with a working distance of 10 mm and an accelerating voltage of 15 kV. Transmission electron microscopy (TEM; Tecnai, Twin 200KV, FEI, Eindhoven, The Netherlands) was utilized to analyze the internal structure and size of the developed COF-Gem.

2.5. In Vitro Release Study of Gem-Loaded COF

The % cumulative release of Gem from Gem-loaded COF were examined at pH 5.0 and pH 7.4 to mimic the extracellular physiological characteristics of cancer cells and normal cells, respectively. COF-Gem with a concentration of 10 mg/mL in respective media were incubated at 37 °C for 72 h with continuous shaking (IKA® orbital matrix shaker, Delta F2.0, Staufenim Breisgau, Germany). The concentration of Gem released at predetermined time intervals was monitored by HPLC, and after each sampling, the same volume of fresh media was added to the solution.

2.6. In Vitro Biocompatibility and Cytotoxicity Evaluation of COF and COF-Gem Using MTT Cell Viability Assay

To determine the biocompatibility of COF, MTT assay was performed at 48 h. Safety evaluation COF was performed in L929 fibroblasts, and the toxicity of COF-Gem was assessed in MIA-PaCa-2 and PANC-1 cells. Briefly, 5000 cells/well were seeded in 96-well

plates and allowed to attain confluency and desired shape. The cells were then treated with COF (10, 20, 50, 100, 200 μg) and COF-Gem (0.5, 1, 5, 10, 25 μM). The medium was withdrawn after 48 h, and MTT was added. The mixture was incubated at 37 °C, 5% CO_2, and absorbance was measured at 570 nm [26–31]. The % cell viability relative to the control was calculated using the following formula:

$$\%\ Cell\ viability = \frac{OD_{test}}{OD_{control}} \times 100$$

2.7. Statistical Analysis

Each experiment was carried out in triplicate, and the mean ± standard deviation (SD) was used to express the results obtained in the study. GraphPad Prism 10 (GraphPad Software Inc., Solana Beach, CA, USA) was used for analyzing all data using one-way analysis of variance (ANOVA) and Tukey's post hoc test at a statistical significance level of $p < 0.05$.

3. Result and Discussion

3.1. Synthesis and Characterization of COF

Imine-linked COFs have demonstrated exceptional hydrolytic stability compared to boronate ester COFs and remain stable in various organic solvents, even under acidic or basic conditions. Additionally, due to presence of a lone pair of electrons on the nitrogen atom of imine, they act as a Schiff base and may coordinate with a Gem through interactions such as hydrogen bonding and coordination bonds [32]. The imine-linked COF was synthesized from 1,3,5-Triformylbenzene and o-Dianisidine through the solvothermal method in 1,4-dioxane solvent and 3M acetic acid at 120 °C for three days (Scheme 1) [25]. The synthesized COF was not soluble in organic solvents like hexane, N, N-dimethylformamide, dimethyl sulfoxide, acetone, tetrahydrofuran, etc.

The FTIR analysis was conducted to confirm the synthesis of imine-linked COF from the starting materials (i.e., 1,3,5-Triformylbenzene and o-dianisidine) (Figure 1). Upon examination of spectra, it was found that the synthesized compound exhibited distinct structural characteristics compared to the starting materials. The NH stretching broad peak was observed at 3400–3500 cm^{-1} for o-dianisidine, and the C=O stretching peak of 1,3,5-Triformylbenzene was observed at 1691 cm^{-1}. In the FTIR spectra of COF, both the peaks of the starting materials, i.e., (1,3,5-Triformylbenzene (1691 cm^{-1}) and o-dianisidine (3400–3500 cm^{-1}) were mostly attenuated, and a new peak at 1616 cm^{-1} was observed corresponding to CN stretching vibration [33]. The peak at 2915–2846 cm^{-1} in the spectrum of COF corresponded to C-H stretching vibration, and out-of-plane stretching C-H vibrational bands were observed at 900–675 cm^{-1}. These results indicate that the imine-linked COF was successfully synthesized from the starting materials [34].

3.2. Estimation of Drug Loading and Characterization of Synthesized COF-Gem

The loading of Gem in COF was determined to be 30 μg/mg using high-performance liquid chromatography (HPLC), which is significantly higher than other carrier systems (Supporting Information Figure S1). For instance, in a study, Gem-loaded PLGA-PEG nanoparticles exhibited a loading capacity of 7 μg/mg for Gem, whereas in another study, Gem-loaded PEGylated PLGA nanoparticles co-encapsulated with anti-sense miRNA21 demonstrated a loading capacity of 2.1%. The solid lipid nanoparticles of Gem demonstrated loading efficiency ranges between 0.7% and 1.2%. Moreover, native PLGA nanospheres display much lower efficiencies, ranging from 0.007% to 0.03% [35–38].

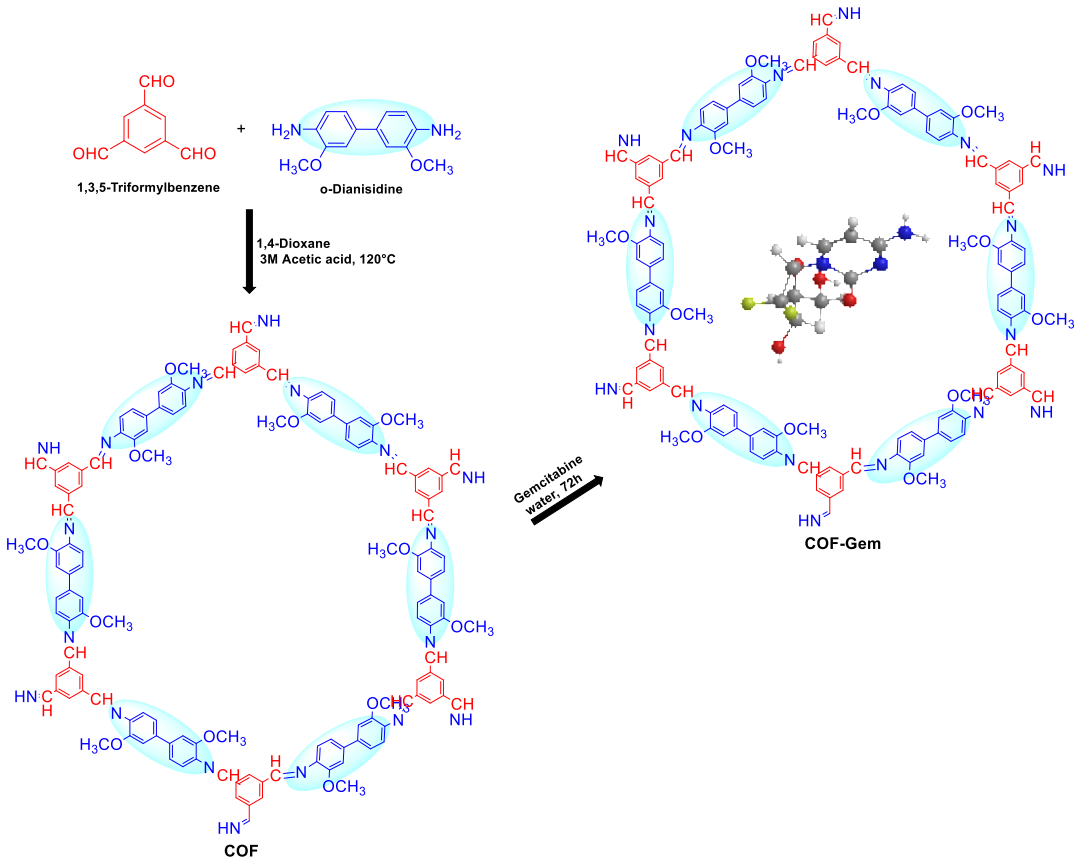

Scheme 1. Synthetic scheme for the synthesis of COF from 1,3,5-Triformylbenzene and o-Dianisidine and loading of gemcitabine in synthesized COF carrier system.

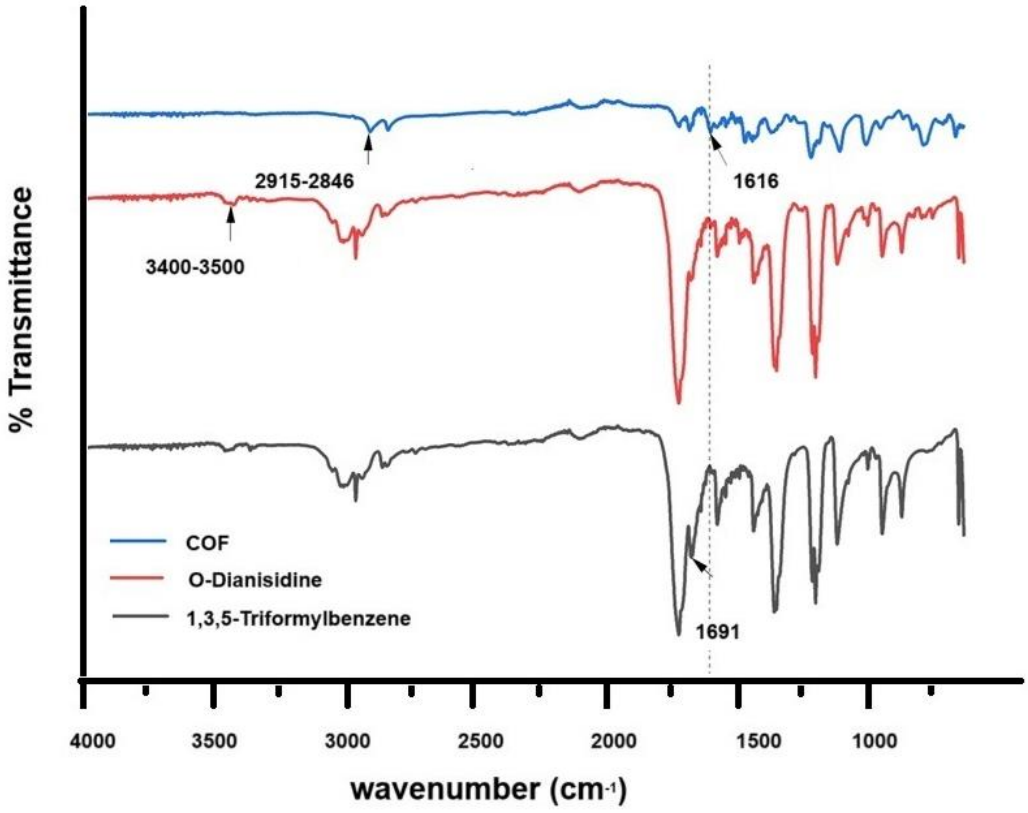

Figure 1. FTIR spectra of COF (blue), o-Dianisidine (red), and 1,3,5 Triformylbenzene (black).

The spectra of COF, Gem, and COF-Gem were examined to elucidate the interactions between COF and Gem. As depicted in Figure 2a, the spectra of Gem display a broad peak in the 3103–3404 cm^{-1} range, corresponding to OH and NH stretching vibrations, along with a peak at 1691–1609 cm^{-1}, attributed to amine bending and C=O stretching vibrations [39]. In the FTIR spectrum of COF-Gem, the distinctive peaks of COF remained unchanged, but a new peak at 3363 cm^{-1}, corresponding to the NH and OH stretching vibrations of Gem, appeared with reduced intensity. Additionally, an increase in the intensity of C=O and C≡N stretching vibrations was noted in the COF-Gem spectrum, likely due to overlapping with Gem's peaks.

Furthermore, TGA was employed to determine the thermal stability of COF (Figure 2b). The TGA curve clearly indicated the initial thermal degradation up to 350 °C with a main reduction in weight resulting from disintegration after 400 °C, demonstrating higher thermal stability of COF. It can be inferred that the aromatic structure started to carbonize as the temperature increased, and 50% of the starting mass was stable at 600 °C [40].

The TGA thermogram of COF-Gem showed two significant weight loss phases: the first between 300 and 500 °C and the second between 500 and 700 °C, which correspond to the decomposition of COF (Figure 2b) [35]. The morphology of COF was investigated through scanning electron microscopy and transmission electron microscopy. The SEM image of COF displays the spherical particles (Supporting Information Figure S2). In comparison, the SEM image of Gem-loaded COF (Figure 2c) shows a higher degree of integration of these spherical particles compared to the blank COF. Similarly, the TEM image of COF-Gem corroborates the SEM findings, confirming a spherical morphology (Figure 2d) [41]. These observations collectively confirm the successful encapsulation of Gem within the COF.

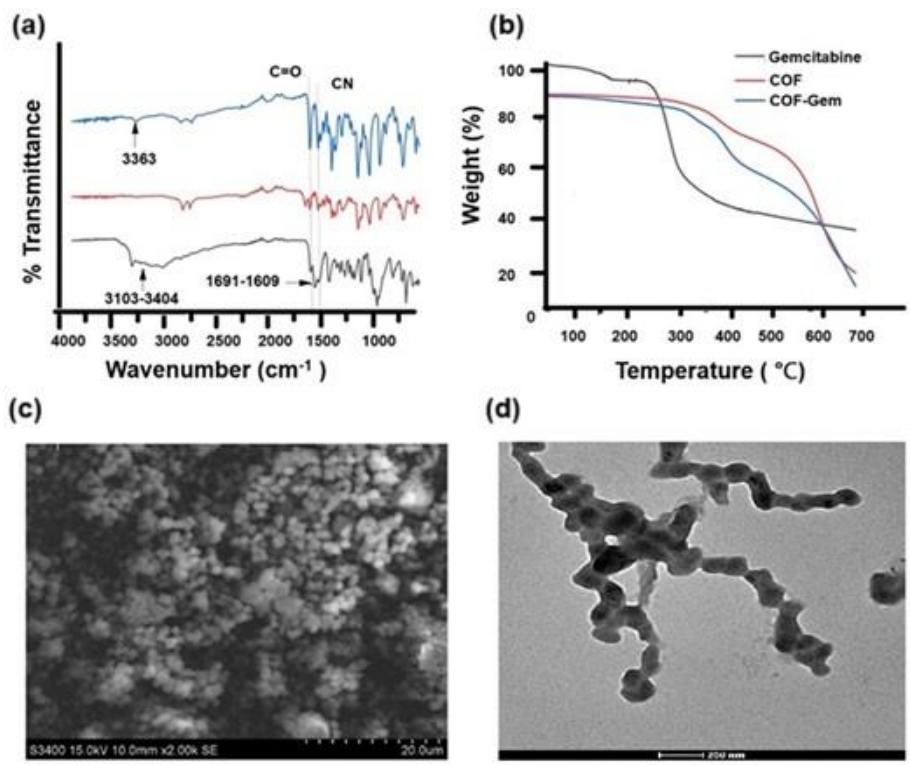

Figure 2. Characterization of COF and COF-Gem. (**a**) FT-IR and (**b**) TGA spectra of Gem (black) COF (red), and COF-Gem (blue). The morphology of COF-Gem using (**c**) SEM and (**d**) TEM.

3.3. In Vitro Release Study of Gem from COF-Gem

The cumulative release of encapsulated therapeutic agents from carrier systems depends on various conditions. In this study, the in vitro cumulative release of Gem from COF-Gem was evaluated at pH 7.4 and pH 5.0 to assess the impact of pH. The release rate at pH 5.0 was higher than at pH 7.4, which may be due to the weakening interaction between Gem and COF in acidic medium. A burst release effect was observed for COF-Gem within the first hour, followed by a sustained and controlled release over 72 h (Figure 3). This initial burst may be attributed to Gem molecules remaining on the surface of the COF without strong interactions [25].

The results indicated that at pH 7.4, the release of Gem from COF was 25 ± 1.1%, whereas at pH 5, it increased to 48 ± 2.5% over 72 h. These data demonstrate a significantly slower, continuous, and sustained release from COF-Gem. The in vitro release studies confirmed that the synthesized COF carrier is effective for drug delivery systems, capable of providing prolonged therapeutic effects when used as a carrier for anticancer drugs. These findings suggest that the newly synthesized COF acts as a pH-responsive drug delivery vehicle, minimizing drug release at the physiological pH of normal cells and accelerating drug release at the more acidic target site (pH 5.0). As a result, COF-Gem could facilitate controlled drug release, potentially reducing the side effects associated with cancer treatments.

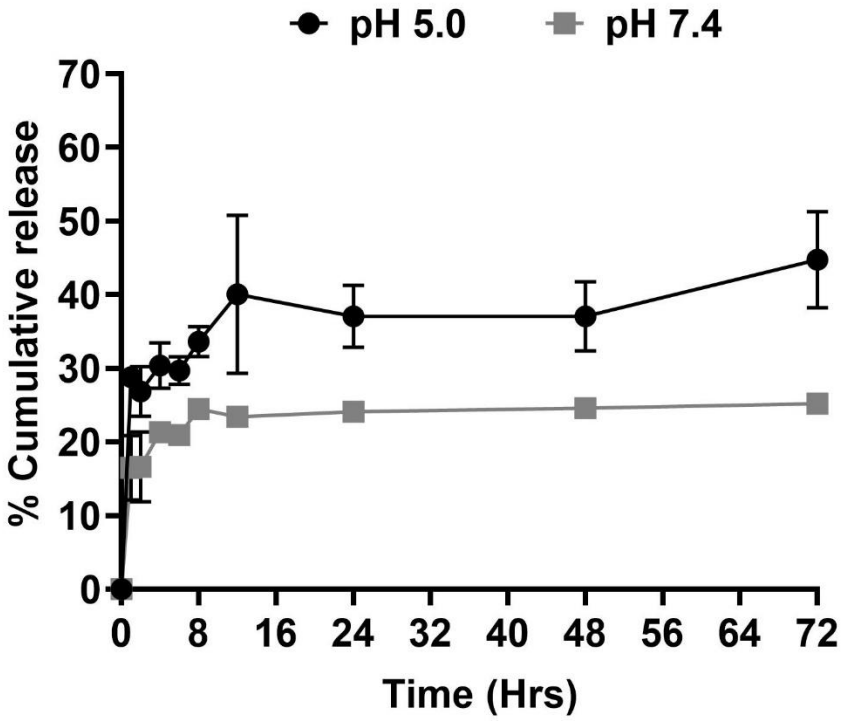

Figure 3. In vitro release profiles of Gem from COF-GEM at pH 7.4 and 5.0 expressed as percent cumulative release recorded till 72 h.

3.4. Examination of Cell Viability via MTT Assay

The biocompatibility of the COF was first determined on L929 (mouse fibroblast cell line) through MTT cell viability assay. The COF showed negligible cell death across the 0–200 μg/mL concentration range up to 48 h (Supporting Information Figure S3). Even at the highest concentration of 200 μg/mL, 90% cell were viable, indicating the safety of the COF. Further, to identify the effect of COF-Gem on pancreatic cancer cell lines (MIA-PaCa-2 and PANC-1), the cells were treated with COF-Gem for 48 h (Figure 4). The results demonstrated significant reductions in cellular proliferation at all treatments levels

compared to the control. The half-maximal inhibitory concentration (IC_{50}) values of Gem and COF-Gem are given in Table 1.

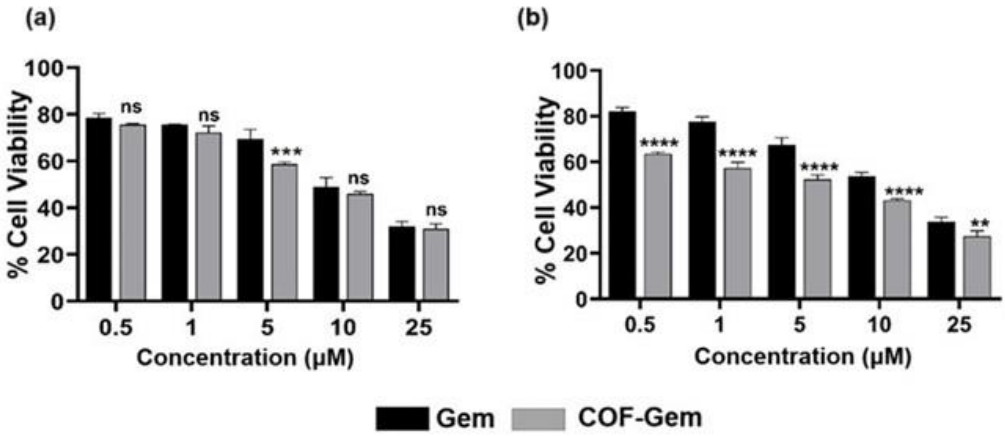

Figure 4. Effect of Gem and COF-Gem in MIA-PaCa-2 and PANC-1 cell lines measured via MTT essay. (**a**) Cell viability graph of MIA-PaCa-2 cells after 48 h treatment at different concentrations (0.5, 1, 5, 10, and 25 μM). (**b**) Cell viability graph of PANC-1 cells after 48 h treatment at different concentrations (0.5, 1, 5, 10, and 25 μM). **** $p < 0.0001$, *** $p < 0.001$, and ** $p < 0.01$ indicate significant differences in the mean value compared to GEM. ns: non-significant.

Table 1. IC_{50} values (μM) of Gem and COF-Gem in two different cell lines (MIA-PaCa-2, PANC-1) for 48 h.

Compound	MIA-PaCa-2	PANC-1
Gem	10.7 ± 0.8	11.8 ± 0.7
COF-Gem	8.1 ± 1.2 *	6.0 ± 1.3 ***

*** $p < 0.001$ and * $p < 0.05$ indicate significant differences in the mean value compared to GEM.

4. Conclusions

A 2D imine-linked COF was successfully synthesized and employed as a carrier system for Gem delivery with a higher drug loading of 30 μg/mg. The COF-Gem demonstrated a pH-dependent release of GEM with a sustained release profile in acidic pH. In vitro biocompatibility studies indicated minimal toxicity of the unloaded COF, even at higher concentrations (200 μg/mL), highlighting its suitability for biomedical applications. In contrast, the Gem-loaded COF showed better cytotoxic effects, with IC_{50} values of 8.1 ± 1.2 μM against MIA-PaCa-2 cells and 6.0 ± 1.3 μM against PANC-1 cells after 48 h of treatment. In summary, our findings demonstrate that COFs hold significant promise as delivery systems for hydrophilic drugs, offering higher drug-loading capacity and enhanced therapeutic efficacy.

Supplementary Materials: The following supporting information can be downloaded at: https://www.mdpi.com/article/10.3390/colloids9010008/s1, Figure S1: (a) Stacked chromatogram of Gemcitabine at various concentrations. (b) Standard calibration curve of Gemcitabine used for deducing the loading of Gem in COF; Figure S2: SEM image of COF; Figure S3: Cell viability graph of (a) L929, (b) PANC-1, (c) MIA-PaCa-2 cells after 48 h treatment at different concentrations (10, 20, 50, 100, 200 μg/mL).

Author Contributions: K.K.: writing—original draft, methodology, formal analysis. N.B.: writing—original draft, methodology, formal analysis. R.: writing—original draft, methodology, formal analysis. A.S.: writing—review and editing, supervision, project administration, funding acquisition, conceptualization. All authors have read and agreed to the published version of the manuscript.

Funding: The authors acknowledge the financial assistance received from CSIR (MLP204).

Data Availability Statement: The data presented in this study are included in the article. Further inquiries can be directed to the corresponding author.

Acknowledgments: The authors are grateful to Palampur of CSIR-IHBT, for his continuous support and encouragement. A.S. acknowledges the financial assistance from CSIR (MLP204). K.K. acknowledges the University Grants Commission (UGC) for providing the senior research fellowship (SRF). N. B. is grateful to the Indian Council of Medical Research (ICMR), New Delhi (File no. 3/1/2/220/2021-Nut.), for the fellowship. The Council of Scientific and Industrial Research (CSIR), New Delhi, is acknowledged by R. for the fellowship (File 31/054(0163)/2020-EMR-I). The Authors acknowledge the National Institute of Pharmaceutical Education and Research, Hyderabad, for performing TGA and FTIR analyses. This manuscript bears the institutional communication number 5716.

Conflicts of Interest: The authors declare that they have no known competing financial interests or personal relationships that could have appeared to influence the work reported in this paper.

References

1. Akhtar, M.J.; Ahamed, M.; Alhadlaq, H.A.; Alrokayan, S.A.; Kumar, S. Targeted anticancer therapy: Overexpressed receptors and nanotechnology. *Clin. Chim. Acta* **2014**, *436*, 78–92. [CrossRef] [PubMed]
2. Torchilin, V.P. Drug targeting. *Eur. J. Pharm. Sci.* **2000**, *11*, S81–S91. [CrossRef] [PubMed]
3. Pradhan, S.; Mishra, A.; Sahoo, S.; Pradhan, S.; Babu, P.J.; Singh, Y.D.; Chanu, N.B. Artemisinin based nanomedicine for therapeutic applications: Recent advances and challenges. *Pharmacol. Res. Mod. Chin. Med.* **2022**, *2*, 100064. [CrossRef]
4. Liu, Z.; Chen, K.; Davis, C.; Sherlock, S.; Cao, Q.; Chen, X.; Dai, H. Drug delivery with carbon nanotubes for in vivo cancer treatment. *Cancer Res.* **2008**, *68*, 6652–6660. [CrossRef] [PubMed]
5. Zhuang, J.; Kuo, C.-H.; Chou, L.-Y.; Liu, D.-Y.; Weerapana, E.; Tsung, C.-K. Optimized metal–organic-framework nanospheres for drug delivery: Evaluation of small-molecule encapsulation. *ACS Nano* **2014**, *8*, 2812–2819. [CrossRef]
6. Hong, G.; Diao, S.; Antaris, A.L.; Dai, H. Carbon nanomaterials for biological imaging and nanomedicinal therapy. *Chem. Rev.* **2015**, *115*, 10816–10906. [CrossRef]
7. Arruebo, M. Drug delivery from structured porous inorganic materials. *Wiley Interdiscip. Rev. Nanomed. Nanobiotechnol.* **2012**, *4*, 16–30. [CrossRef]
8. Zhang, G.; Li, X.; Liao, Q.; Liu, Y.; Xi, K.; Huang, W.; Jia, X. Water-dispersible PEG-curcumin/amine-functionalized covalent organic framework nanocomposites as smart carriers for in vivo drug delivery. *Nat. Commun.* **2018**, *9*, 2785. [CrossRef]
9. Khan, N.; Slathia, G.; Kaliya, K.; Saneja, A. Recent progress in covalent organic frameworks for cancer therapy. *Drug Discov. Today* **2023**, *28*, 103602. [CrossRef]
10. Cote, A.P.; Benin, A.I.; Ockwig, N.W.; O'Keeffe, M.; Matzger, A.J.; Yaghi, O.M. Porous, crystalline, covalent organic frameworks. *Science* **2005**, *310*, 1166–1170. [CrossRef]
11. Machado, T.F.; Serra, M.E.S.; Murtinho, D.; Valente, A.J.; Naushad, M. Covalent organic frameworks: Synthesis, properties and applications—An overview. *Polymers* **2021**, *13*, 970. [CrossRef] [PubMed]
12. Geng, K.; He, T.; Liu, R.; Dalapati, S.; Tan, K.T.; Li, Z.; Tao, S.; Gong, Y.; Jiang, Q.; Jiang, D. Covalent organic frameworks: Design, synthesis, and functions. *Chem. Rev.* **2020**, *120*, 8814–8933. [CrossRef] [PubMed]
13. Akinnawo, S.O. Covalent organic frameworks: Design, synthesis, characterization, and applications. *ChemPhysMater* **2024**, *3*, 36–63. [CrossRef]
14. Lohse, M.S.; Bein, T. Covalent organic frameworks: Structures, synthesis, and applications. *Adv. Funct. Mater.* **2018**, *28*, 1705553. [CrossRef]
15. Diercks, C.S.; Yaghi, O.M. The atom, the molecule, and the covalent organic framework. *Science* **2017**, *355*, eaal1585. [CrossRef]
16. Ding, S.-Y.; Wang, W. Covalent organic frameworks (COFs): From design to applications. *Chem. Soc. Rev.* **2013**, *42*, 548–568. [CrossRef]
17. El-Kaderi, H.M.; Hunt, J.R.; Mendoza-Cortés, J.L.; Côté, A.P.; Taylor, R.E.; O'Keeffe, M.; Yaghi, O.M. Designed synthesis of 3D covalent organic frameworks. *Science* **2007**, *316*, 268–272. [CrossRef]
18. Liu, R.; Tan, K.T.; Gong, Y.; Chen, Y.; Li, Z.; Xie, S.; He, T.; Lu, Z.; Yang, H.; Jiang, D. Covalent organic frameworks: An ideal platform for designing ordered materials and advanced applications. *Chem. Soc. Rev.* **2021**, *50*, 120–242. [CrossRef]
19. Bai, L.; Phua, S.Z.F.; Lim, W.Q.; Jana, A.; Luo, Z.; Tham, H.P.; Zhao, L.; Gao, Q.; Zhao, Y. Nanoscale covalent organic frameworks as smart carriers for drug delivery. *Chem. Commun.* **2016**, *52*, 4128–4131. [CrossRef]

20. Vyas, V.S.; Vishwakarma, M.; Moudrakovski, I.; Haase, F.; Savasci, G.; Ochsenfeld, C.; Spatz, J.P.; Lotsch, B.V.J.A.M. Exploiting noncovalent interactions in an imine-based covalent organic framework for quercetin delivery. *Adv. Mater* **2016**, *28*, 8749–8754. [CrossRef]
21. Huang, N.; Wang, P.; Jiang, D. Covalent organic frameworks: A materials platform for structural and functional designs. *Nat. Rev. Mater.* **2016**, *1*, 1–19. [CrossRef]
22. Fang, Q.; Wang, J.; Gu, S.; Kaspar, R.B.; Zhuang, Z.; Zheng, J.; Guo, H.; Qiu, S.; Yan, Y. 3D porous crystalline polyimide covalent organic frameworks for drug delivery. *J. Am. Chem. Soc.* **2015**, *137*, 8352–8355. [CrossRef] [PubMed]
23. Mitra, S.; Sasmal, H.S.; Kundu, T.; Kandambeth, S.; Illath, K.; Diaz Diaz, D.; Banerjee, R. Targeted drug delivery in covalent organic nanosheets (CONs) via sequential postsynthetic modification. *J. Am. Chem. Soc.* **2017**, *139*, 4513–4520. [CrossRef] [PubMed]
24. Kaliya, K.; Bhardwaj, N.; Satwalia, R.; Saneja, A. Synthesis of a Gemcitabine Prodrug and its Encapsulation into Polymeric Nanoparticles for Improved Therapeutic Efficacy. *ChemMedChem* **2025**, e202400532. [CrossRef]
25. Akyuz, L.J.M. An imine based COF as a smart carrier for targeted drug delivery: From synthesis to computational studies. *Microporous Mesoporous Mater.* **2020**, *294*, 109850. [CrossRef]
26. Jia, Y.; Zhang, L.; He, B.; Lin, Y.; Wang, J.; Li, M. 8-Hydroxyquinoline functionalized covalent organic framework as a pH sensitive carrier for drug delivery. *Mater. Sci. Eng. C* **2020**, *117*, 111243. [CrossRef]
27. Zhao, K.; Gong, P.; Huang, J.; Huang, Y.; Wang, D.; Peng, J.; Shen, D.; Zheng, X.; You, J.; Liu, Z. Fluorescence turn-off magnetic COF composite as a novel nanocarrier for drug loading and targeted delivery. *Microporous Mesoporous Mater.* **2021**, *311*, 110713. [CrossRef]
28. Ma, B.; Xu, Y.; Hu, F.; Zhai, L.; Huang, Y.; Qiao, H.; Xiong, J.; Yang, D.; Ni, Z.; Zheng, X. Fluorinated covalent organic frameworks for efficient drug delivery. *RSC Adv.* **2022**, *12*, 31276–31281. [CrossRef]
29. Li, M.; Peng, Y.; Yan, F.; Li, C.; He, Y.; Lou, Y.; Ma, D.; Li, Y.; Shi, Z.; Feng, S. A cage-based covalent organic framework for drug delivery. *New J. Chem.* **2021**, *45*, 3343–3348. [CrossRef]
30. Ma, J.; Hui, P.; Meng, W.; Wang, N.; Xiang, S. Ku70 inhibits gemcitabine-induced DNA damage and pancreatic cancer cell apoptosis. *Biochem. Biophys. Res. Commun.* **2017**, *484*, 746–752. [CrossRef]
31. Bimonte, S.; Leongito, M.; Barbieri, A.; Del Vecchio, V.; Barbieri, M.; Albino, V.; Piccirillo, M.; Amore, A.; Di Giacomo, R.; Nasto, A. Inhibitory effect of (−)-epigallocatechin-3-gallate and bleomycin on human pancreatic cancer MiaPaca-2 cell growth. *Infect. Agents Cancer* **2015**, *10*, 1–7. [CrossRef] [PubMed]
32. Huang, T.; Zhang, W.; Yang, S.; Wang, L.; Yu, G. Imine-linked covalent organic frameworks: Recent advances in design, synthesis, and application. *SmartMat* **2024**, *5*, e1309. [CrossRef]
33. Alsudairy, Z.; Brown, N.; Yang, C.; Cai, S.; Akram, F.; Ambus, A.; Ingram, C.; Li, X. Facile microwave-assisted synthesis of 2D imine-linked covalent organic frameworks for exceptional iodine capture. *Precis. Chem.* **2023**, *1*, 233–240. [CrossRef] [PubMed]
34. Ding, S.-Y.; Gao, J.; Wang, Q.; Zhang, Y.; Song, W.-G.; Su, C.-Y.; Wang, W. Construction of covalent organic framework for catalysis: Pd/COF-LZU1 in Suzuki–Miyaura coupling reaction. *J. Am. Chem. Soc.* **2011**, *133*, 19816–19822. [CrossRef] [PubMed]
35. Affram, K.O.; Smith, T.; Ofori, E.; Krishnan, S.; Underwood, P.; Trevino, J.G.; Agyare, E. Cytotoxic effects of gemcitabine-loaded solid lipid nanoparticles in pancreatic cancer cells. *J. Drug Deliv. Sci. Technol.* **2020**, *55*, 101374. [CrossRef]
36. Saneja, A.; Kumar, R.; Mintoo, M.J.; Dubey, R.D.; Sangwan, P.L.; Mondhe, D.M.; Panda, A.K.; Gupta, P.N. Gemcitabine and betulinic acid co-encapsulated PLGA−PEG polymer nanoparticles for improved efficacy of cancer chemotherapy. *Mater. Sci. Eng. C* **2019**, *98*, 764–771. [CrossRef]
37. Devulapally, R.; Foygel, K.; Sekar, T.V.; Willmann, J.K.; Paulmurugan, R. Gemcitabine and antisense-microRNA co-encapsulated PLGA–PEG polymer nanoparticles for hepatocellular carcinoma therapy. *ACS Appl. Mater. Interfaces* **2016**, *8*, 33412–33422. [CrossRef]
38. Jaidev, L.; Krishnan, U.M.; Sethuraman, S. Gemcitabine loaded biodegradable PLGA nanospheres for in vitro pancreatic cancer therapy. *Mater. Sci. Eng. C* **2015**, *47*, 40–47. [CrossRef]
39. Jamil, A.; Aamir Mirza, M.; Anwer, M.K.; Thakur, P.S.; Alshahrani, S.M.; Alshetaili, A.S.; Telegaonkar, S.; Panda, A.K.; Iqbal, Z. Co-delivery of gemcitabine and simvastatin through PLGA polymeric nanoparticles for the treatment of pancreatic cancer: In-vitro characterization, cellular uptake, and pharmacokinetic studies. *Drug Dev. Ind. Pharm.* **2019**, *45*, 745–753. [CrossRef]
40. Li, Z.; Feng, X.; Zou, Y.; Zhang, Y.; Xia, H.; Liu, X.; Mu, Y. A 2D azine-linked covalent organic framework for gas storage applications. *Chem. Commun.* **2014**, *50*, 13825–13828. [CrossRef]
41. Wang, Y.; Xie, J.; Ren, Z.; Guan, Z.-H. Postsynthetically modified hydrophobic covalent organic frameworks for enhanced oil/water and CH_4/C_2H_2 separation. *Chem. Eng. J.* **2022**, *448*, 137687. [CrossRef]